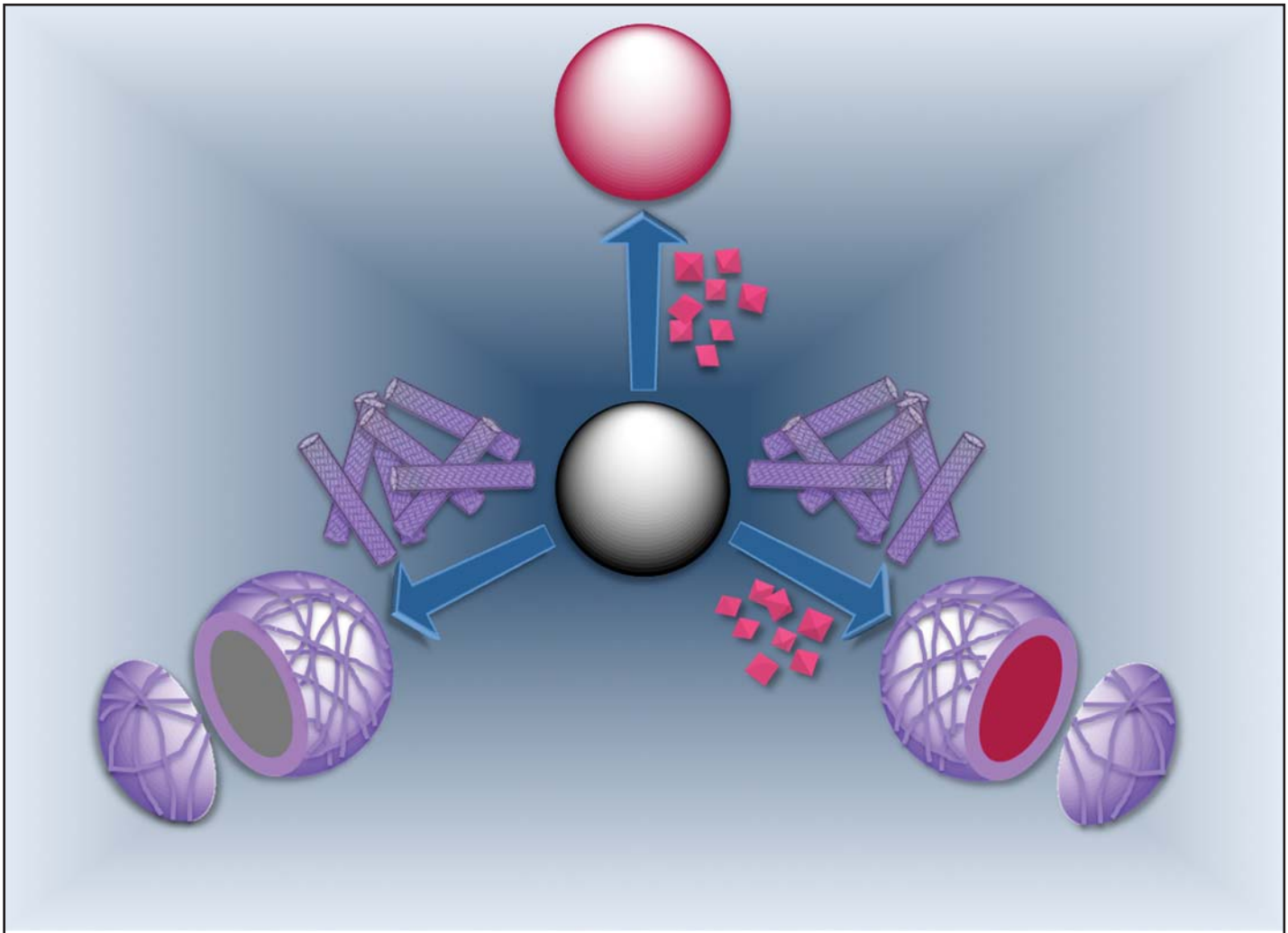

Showcasing research from Angel Martí's laboratory, Rice University, USA, http://www.owlnet.rice.edu/~amarti/Home.html

Title: Single-walled carbon nanotubes shell decorating porous silicate materials: A general platform for studying the interaction of carbon nanotubes with photoactive molecules

Single-Walled Carbon Nanotubes are immobilized in the external surface of porous silicate materials by deposition from chlorosulfonic acid. Photoinduced electron transfer reactions between ruthenium complexes within the pores and SWCNTs in the external surface are demonstrated.

As featured in:

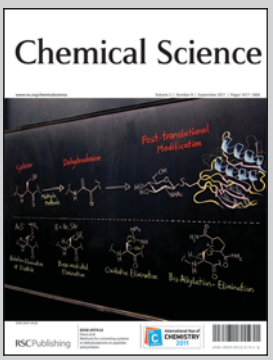

See Avishek Saha, Saunab Ghosh, Natnael Behabtu, Matteo Pasquali and Angel A. Martí, *Chem. Sci.*, 2011, **2**, 1682.

RSC Publishing

www.rsc.org/chemicalscience

Registered Charity Number 207890

Chemical Science

Dynamic Article Links

Cite this: *Chem. Sci.*, 2011, **2**, 1682

www.rsc.org/chemicalscience

EDGE ARTICLE

Single-walled carbon nanotubes shell decorating porous silicate materials: A general platform for studying the interaction of carbon nanotubes with photoactive molecules†

Avishek Saha,[ac] Saunab Ghosh,[ac] Natnael Behabtu,[cd] Matteo Pasquali[acd] and Angel A. Martí*[abc]

Received 26th May 2011, Accepted 17th June 2011
DOI: 10.1039/c1sc00323b

Single-walled carbon nanotubes (SWCNTs) have been deposited onto the external surface of porous silicate materials by deposition from a solution of individualized, protonated SWCNTs in chlorosulfonic acid. It is demonstrated that the deposited SWCNTs can be deprotonated on the silicate surface, yielding a microporous or mesoporous material with individual or small bundles of SWCNTs. These carbon nanotubes present all the spectral characteristics of pristine SWCNTs, including van Hove transitions, Raman and NIR photoluminescence. Furthermore, it is shown that these materials can be used as scaffolds to study the interaction of SWCNTs with photoactive molecules loaded in the cavities of the porous silicate materials. As a proof-of-concept, we showed that the photoluminescence of tris(2,2′-bipyridine)ruthenium(II) can be quenched by protonated SWCNTs in the nearby surface decreasing its lifetime by nearly two orders of magnitude. This represents a novel application for these materials, especially considering the large amount of different molecules that can be immobilized in the internal cavities of these porous silicates.

Introduction

Carbon nanotubes (CNTs) are one of the most studied substances of the last two decades.[1–6] The single-walled version (SWCNTs),[7,8] are quasi one-dimensional structures, which can be viewed as rolled graphene sheets. Due to their distinctive structure, SWCNTs possess unique electronic, optical and mechanical properties.[1,9–11] Their assembly into large-scale functional materials requires addressing important challenges, including their organization, alignment and individualization.[10,12] Furthermore, finding platforms that would allow the study of the interaction of SWCNTs with a variety of molecules is of fundamental importance. Overcoming these challenges is one of the main and still more elusive goals of carbon nanotechnology.

SWCNTs on the surfaces of microparticles have important applications as stationary phases for chromatography,[13–16] sensors,[17] and formation of carbon microstructures such as carbon microspheres.[15,18] We have chosen the porous silicates zeolite-Y and MCM-41 as substrates for the immobilization of SWCNTs. Zeolites are crystalline microporous materials with defined pore structures.[19] The zeolite framework is composed of silicon atoms tetrahedrally coordinated by oxygen and linked together forming a porous silicate structure. Commonly, some of the silicon atoms are substituted by aluminum, imparting an intrinsic negative charge to the site. This charge is stabilized by a cation, generally sodium, although any alkali or alkaline earth can act as the counterion of these negative sites.[20] Due to their channel structure, ion-exchange properties, and molecular and size recognition, many ions and molecules have been immobilized within zeolites channels.[21–26] MCM-41 is also a silicate material such as zeolites, but with larger pores and a less crystalline structure. In this work we report how to efficiently cover the external surface of silicates (Zeolite-Y and MCM-41) with different pore sizes, framework structures and aluminum content with SWCNTs (Fig. 1). The SWCNTs dispersed on the surface are immobilized and individualized without the assistance of any wrapping molecules such as surfactants. Furthermore, we present experimental evidence that protonated SWCNTs can be converted back to pristine nanotubes with a full recovery of their photophysical properties, including van-Hove transitions and

[a]*Department of Chemistry, MS-60, Rice University, 6100 S. Main Street, Houston, TX, 77005, USA. E-mail: amarti@rice.edu; Fax: +1-713-348-5155; Tel: +1-713-348-3486*
[b]*Department of Bioengineering, Rice University, Houston, TX, 77005, USA*
[c]*Smalley Institute for Nanoscale Science and Technology, Rice University, Houston, TX, 77005, USA*
[d]*Department of Chemical and Biomolecular Engineering, Rice University, Houston, TX, 77005, USA*

† Electronic supplementary information (ESI) available: UV-Vis of SWCNTs in superacid solution, Raman of diethyl ether treated pSWCNTs@MCM-41, Raman of vpSWCNTs@MCM-41 0.67% (w/w) and 1.3% (w/w), TEM elemental mapping of pSWCNTs@MCM-41, TEM microscopy figures and discussion, Photoluminescence spectra of Ru-MCM-41 and Ru-pSWCTNs@MCM-41. See DOI: 10.1039/c1sc00323b

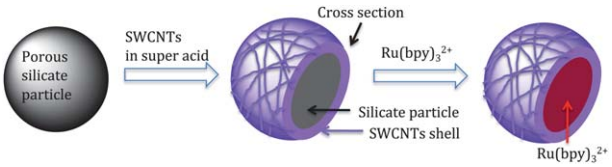

Fig. 1 Pictorial representation of the deposition of SWCNTs onto the external surface of a porous silicate material and the subsequent loading of the photoactive molecule Ru(bpy)$_3^{2+}$ within the pores of the silicate particle.

photoluminescence. Finally, we show that molecules can be loaded into the cavities of these materials (specifically tris-(2-2′bipyridine) ruthenium(II), (Ru(bpy)$_3^{2+}$) conveniently allowing the study of the interaction of SWCNTs with molecules in the pores without further chemical modification of the molecules or the SWCNTs.

Materials and methods

HiPco SWCNTs were purified as described elsewhere.[27] MCM-41-A was obtained from Aldrich and MCM-41-B was synthesized as described by Ryoo, *et al.*[28] Both samples were characterized by nitrogen adsorption isotherm and powder X-ray diffraction (ESI,† Fig. S6 and S7, respectively). In a typical SWCNT deposition experiment, 1–4 mg SWCNT are placed in a vacuum oven at 110 °C for 12 h. Following this, SWCNTs were dissolved in 6 mL of chlorosulfonic acid (inside glove box) and stirred for 24 h. Then, the calcined MCM-41/NaY/USY was added to the SWCNTs solution. After 24 h at constant stirring, the mixture was filtered (2.0 μM PTFE supported Zefluor™) and the supernatant collected and analyzed by UV-Vis spectroscopy (Shimatzu UV-2450) using 1 cm pathlength quartz cells. The supernatants were diluted by a factor of 20 before absorption measurements. The concentration of nanotubes remaining in the supernatant was calculated from the UV-Vis absorption intensity at 500 nm as described by Rai *et al.*[29] The concentration of SWCNTs absorbed was calculated by subtracting the concentration in the supernatant from the concentration of SWCNTs before the deposition experiments (calculated also by UV-Vis). These concentrations were used for the construction of the adsorption isotherms. The collected solid was washed three times with pure chlorosulfonic acid and dried at 300 °C for 4 h. The dry samples were kept in a dry inert atmosphere. For vinyl pyrrolidone (VP) treatment, ~50 mg of samples were added to 2 mL of VP and stirred for 30 min followed by bath sonication for 10 s. The samples were then filtrated using 2.0 μm filter paper. Samples were analyzed using a Raman microscope (Renishaw in *Via* MicroRaman Spectrometer). SEM images were obtained on a FEI Quanta 400 ESEM FEG. TEM were obtained using a JEOL 2100 Field Emission Gun Transmission Electron Microscope. Diffuse reflectance was obtained using a UV-Vis spectrometer (Shimadzu UV-2450) equipped with an integrating sphere. Photoluminescence characterizations of SWCNTs were performed in a model NS1 NanoSpectralyzer (Applied NanoFluorescence) from 1050 to 1530 nm relative to matched references (with fixed excitation lasers 638, 687, and 783 nm). One short-pass dielectric filter (FES 1000, Thorlabs) was inserted before the sample compartment to block unwanted longer wavelength excitation lines present in the laser. Another neutral density filter ~42% transmittance was utilized to decrease laser intensity. Loading of Ru(bpy)$_3^{2+}$ into MCM-41 was performed by dissolving 1.32 mg of Ru(bpy)$_3$(PF$_6$)$_2$ in 5 mL of dichloromethane and placing this solution in contact with 200 mg of MCM-41 or pSWCNTs@MCM-41. After two hours, no Ru(bpy)$_3^{2+}$ could be detected in the supernatant solution. Then, the material was filtered and washed thoroughly with dichloromethane, after which the solvent was evaporated. The dry material was used to make a dilute suspension in dichloromethane (0.05% w/V), and purged with ultrapure nitrogen. Time-resolved decays of these suspensions were obtained using an Edinburgh Instruments OD470 single-photon counting spectrometer with a 443.6 nm picosecond pulse diode laser, and monitoring at 620 nm.

Results and discussion

SWCNT deposition onto MCM-41

The first step in the immobilization of individualized CNTs on silicate materials is their individualization in solution. As-synthesized SWCNTs form bundled structures, which are difficult to individualize and bring into solution due to their large cohesive energy (>0.5 eV nm^{-1}).[30] SWCNTs are commonly individualized by sonication in water. Surfactant-stabilized aqueous solutions of SWCNTs (SWCNTs with SDS, cetyl trimethylammonium bromide (CTAB), and pluronic micelles) were placed into contact with MCM-41 and zeolites, showing precipitation of the SWCNTs, and no incorporation on the silicate after 24 h (see ESI, Fig. S10†). A less common, but more effective, method of dissolving SWCNTs as individuals is by using superacids such as fuming sulfuric and chlorosulfonic acids (CSA).[31–33] The solubilization is driven by the protonation of the SWCNTs walls (pSWCNTs), which results in a strong electrostatic inter-SWCNT repulsion. Superacids are a convenient dissolution medium because silicates are stable in them. We dissolved SWCNTs in CSA and placed the solutions in contact with MCM-41-A (SiO_2/Al_2O_3: 80), MCM-41-B (100% SiO_2), and the zeolite-Y materials NaY (SiO_2/Al_2O_3: 5.1) and USY(SiO_2/Al_2O_3: 80). The retention of SWCNTs was followed by UV-Vis spectroscopy of the supernatant after filtration, and absorption isotherms were generated as shown in Fig. 2 (the adsorption isotherms were not followed until saturation because solutions of SWCNTs in CSA above 320 ppm form a gel when in contact with silicates). Subsequent washes with pure CSA did not extract the CNTs from MCM-41. The excess of chlorosulfonic acid not extracted by vacuum filtration was removed by heating at 300 °C, in a furnace under nitrogen atmosphere.

The isotherms in Fig. 2 imply that the composition of the materials plays an important role in their affinity to SWCNTs. MCM-41-B has the lowest affinity towards SWCNTs of all the materials studied. Interestingly, MCM-41-A and -B have a similar pore size (2.9 and 2.2 nm, respectively) and framework structure, differing more substantially in the amount of aluminum present. The zeolite-Y samples, NaY and USY, with SiO_2/Al_2O_3 equal or smaller than MCM-41-A, also show good SWCNTs uptake, which tends to indicate that aluminum content might have a role in the binding of SWCNTs to silicates. In fact,

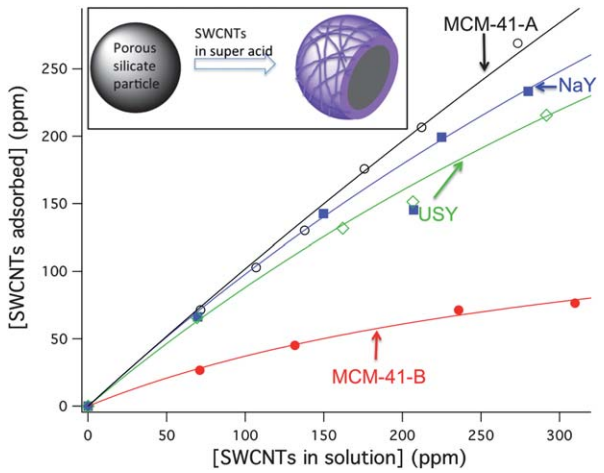

Fig. 2 Adsorption isotherms of SWCNTs with the silicate materials MCM-41-A (—), MCM-41-B (—), NaY (—), and USY (—).

NaY retains slightly more SWCNTs than USY, which is consistent with the higher aluminum content of the former. It is likely that protonated positively charged SWCNTs are attracted to the negatively charged aluminum sites on the surface of aluminosilicates; these aluminum sites can act as counterions for pSWCNTs or participate in proton transfer reactions between pSWCNTs and the aluminosilicate material. Although aluminum sites seem to have a role in modulating the affinity of silicate materials towards SWCNTs, it appears that it is not the only factor. For example, MCM-41-A has a larger SiO_2/Al_2O_3 ratio than NaY, however presented nearly quantitative adsorption at all the concentrations studied. Therefore, other factors such as the surface structure, the size of the external pores, and particle size might have a considerable effect on SWCNTs binding. The effect of silicate particle size on SWCNTs binding is currently under study. The porous silicate particles used in these studies have typical diameters in the range of 200 to 800 nm.

Spectroscopic characterization

In order to thoroughly characterize the produced materials, a set of spectroscopic techniques were used to study the electronic structure of SWCNTs on these silicates. The diffuse reflectance spectrum of pSWCNTs@MCM-41 presented in Fig. 3a lacks the common van Hove transitions that are expected from pristine individual SWCNTs, which is consistent with the UV-Vis spectrum of pSWCNTs in CSA (Fig. S1, ESI†). The optical interband transitions in the UV-Vis are sensitive to the aggregation state of the SWCNTs or to chemical modification. To assess if the absence of van Hove transitions was due to SWCNT bundling or to protonation, Raman spectroscopy was used. The Raman spectrum of pSWCNTs in CSA ($\lambda_{exc.} = 784$ nm) shows only a broad featureless band, which is characteristic of protonated SWCNTs (Fig. 3b). Electromagnetic excitation at 784 nm shows little contribution to the Raman scattering cross section since the electrons responsible for the in-resonance transitions are largely depleted due to the protonation process.[31] The Raman spectrum of pSWCNTs@MCM-41 is similar to the spectrum of pSWCNTs and markedly differs from non-protonated pristine SWCNTs

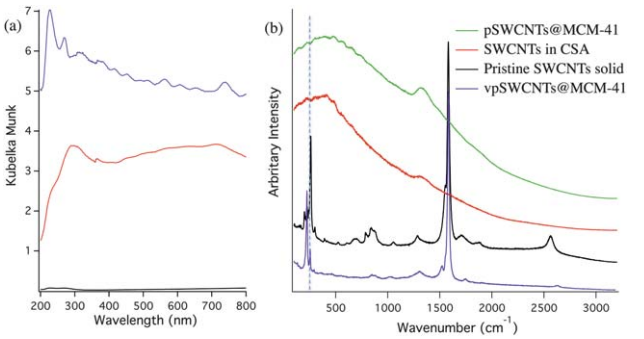

Fig. 3 (a) Diffuse reflectance spectra of vpSWCNTs@MCM-41 0.67% (w/w) (—), pSWCNTs@MCM-41 0.67% (w/w) (—) and mechanically mixed SWCNTs and MCM-41 0.67% (w/w) (—). (b) Raman spectra ($\lambda_{exc.} = 784$ nm) of a pSWCNTs@MCM-41 0.67% (w/w) (—), SWCNTs solution in chlorosulfonic acid (—), pristine SWCNTs powder (—), and vpSWCNTs@MCM-41 0.67% (w/w) (—). Similar spectra are obtained for materials with other SWCNTs@NaY, SWCNTs@USY, and SWCNTs@MCM-41-A and -B with different concentrations of SWCNTs with only variations in their intensities. Dashed line marks the peak at 261 cm^{-1} (roping peak).

(Fig. 3b). This indicates that the removal of CSA from the material leaves protonated SWCNTs on their surface (hereafter, we call these materials pSWCNTs@MCM-41). Furthermore, photoluminescence cannot be observed from pSWCNTs@MCM-41 or pSWCNTs@NaY. The lack of SWCNTs photoluminescence, together with the absence of transitions in Raman and diffuse reflectance indicates that the SWCNTs are still protonated after washing and drying off the CSA.

Once immobilized onto the surface of the porous silicate materials, it would be desirable to deprotonate pSWCNTs to recover a material with individualized pristine SWCNTs; (pristine SWCNTs have more interesting photophysical and electronic properties than functionalized SWCNTs). pSWCNTs can be easily deprotonated using ethyl ether and water.[33] Fig. S2, ESI† shows the Raman spectrum of a sample of pSWCNTs@MCM-41 treated with ethyl ether.[34] Although the common features expected for pristine SWCNTs are recovered, which confirms that SWCNTs are deprotonated, a very intense band at 261 cm^{-1} of comparable intensity to pristine purified SWCNTs is observed. This band is due to the in-resonance Raman transition of (10,2) SWCNTs and is sometimes called the "roping peak" because its intensity has been associated to the degree of aggregation of SWCNTs.[35–37] Therefore, the appearance of this band, of comparable intensity to that of pristine roped SWCNTs, indicates that deprotonation by ethyl ether causes aggregation. Similar results have been obtained with acetone, water and ammonia gas. This strong aggregation is not observed in chlorinated solvents such as dichloromethane and chloroform, which however do not cause deprotonation. In order to deprotonate pSWCNTs immobilized on the surface of silicate materials without inducing aggregation, VP was used. VP has a similar structure as methylpyrrolidone (NMP), that is a solvent commonly used for the dispersion of SWCNTs, however it has a vinyl group that will polymerize in acidic environments to form polyvinylpyrrolidone (PVP). We hypothesized that VP would deprotonate pSWCNTs and at the same time, polymerize on their surface preventing their

aggregation. Fig. 3a shows the diffuse reflectance spectrum of VP treated SWCNTs@MCM-41 (vpSWCNTs@MCM-41) where the van Hove transitions are completely recovered. The recovery of the van Hove transitions not only indicates that the SWCNTs are deprotonated but also individualized. For comparison, we determined the diffuse reflectance of the mechanical mixture of MCM-41-A and bundled pristine SWCNT powders. In this mixture no sharp van Hove transitions can be observed due to the highly bundled state of the nanotubes (Fig. 3a). Furthermore, in the case of mechanical mixture, most of the light is reflected out of the sample and little absorption can be seen, probably due to the fact that the silicate particles, not covered by SWCNTs anymore, reflect most of the light out without absorption.

The Raman spectrum of vpSWCNTs@MCM-41 is also presented in Fig. 3b (see also Fig. S3 and S4, ESI† for an enlargement of the RBA Region), showing recovery of the common features of pristine SWCNTs. Commonly, the ratio between the G band (tangential mode band at *ca.* 1590 cm^{-1}) and the D band (disordered mode at *ca.* 1300 cm^{-1}) is used to assess the integrity of the CNTs sidewalls. A D/G ratio of less than 1/20 is common for HiPco SWCNTs with pristine sidewalls.[38] The D/G ratio of vpSWCNTs@MCM-41 is *ca.* 1/28 (same as pristine SWCNTs not treated with CSA) confirming that pristine SWCNTs are immobilized on the surface of MCM-41 (Fig. 3b). Moreover, the roping peak at 261 cm^{-1} is greatly reduced in intensity in contrast with pristine SWCNTs, indicating that most nanotubes are unbundled (Fig. 3b).[38] This is also consistent with the decrease in broadening and increase in the intensity of the Raman RBM bands (around 225 cm^{-1}, for expanded spectra see Fig. S3, ESI†). Furthermore, the roping peak does not increase in size with increasing the concentration of SWCNTs on the porous silicate materials indicating that aggregation is not dependent on SWCNT concentration, in contrast with other works[16] (Fig. S4, ESI†). SWCNTs@MCM-41 materials of up to 1.3% (w/w) has been prepared that have just marginal SWCNTs aggregation.

The diffuse reflectance and Raman spectra show that vpSWCNTs@MCM-41 materials contain individual and pristine SWCNTs, with intact photophysical properties. Therefore, the solid material vpSWCNTs@MCM-41 should present photoluminescence in the near-infrared region. Reports of photoluminescence from SWCNTs in solid material are not common in the literature and are restricted to sparse SWCNTs deposited on planar glass surfaces or trapped into thin polymeric films.[39,40] Although some preliminary data from one of our laboratories has suggested that the photoluminescence of SWCNTs could be regenerated after protonation[41] here we present conclusive evidence that pSWCNTs can recover their photoluminescence when deprotonated as long as they remain unbundled. Fig. 4 shows the photoluminescence spectra of vpSWCNTs@MCM-41 at different excitations. This photoluminescence is the ultimate proof for individualization (quenching of photoluminescence is highly efficient in SWCNTs bundles) and is in line with the conclusions from Raman and diffuse reflectance. Furthermore, the spectra of vpSWCNTs@MCM-41 match those in NMP dispersions with minor displacement in their bands, which further confirms that the patterns observed are due to SWCNTs photoluminescence.

Quenching of $Ru(bpy)_3^{2+}$ by SWCNTs with MCM-41 as host

Although porous materials with individual SWCNTs on their surface present potential applications in different fields (as was stated in the introduction) we would like to demonstrate how this material can be used for studying the interaction between photoactive molecules and SWCNTs. In the last few years, much interest has been generated in studying the interaction of SWCNTs with photoactive metal complexes such as porphyrins, however this has always required the chemical functionalization of the photoactive species with anchoring groups (that would help in binding to SWCNTs),[42,43] or their direct covalent attachment.[44,45] In this approach, we have decided to take advantage of the supramolecular framework of pSWCNTs@MCM-41 to encapsulate a photoactive metal complex, $Ru(bpy)_3^{2+}$, in close proximity to pSWCNTs. This ruthenium(II) metal complex, that can be excited at 440 nm, and have a broad photoluminescence spectrum with maximum at 620 nm, has been extensively studied, especially for application in light harvesting materials, and it is a potential candidate for the fabrication of hybrid materials with SWCNTs.

$Ru(bpy)_3^{2+}$ was loaded into MCM-41 following the procedure from Bottinelli *et al.* with slight modifications (see experimental section).[46] The steady-state photoluminescence intensity for Ru$(bpy)_3^{2+}$ loaded into pSWCNTs@MCM-41 (Ru-pSWCNTs@MCM-41) decreases, when compared with the same amount of $Ru(bpy)_3^{2+}$ loaded into MCM-41 (no SWCNTs), in consistency with quenching of the excited state by electron transfer to a nearby acceptor (Fig. S9, ESI†). Although the interaction of $Ru(bpy)_3^{2+}$ with electron acceptors is commonly studied by steady-state photoluminescence quenching, in this case, SWCNTs on the surface of the MCM-41 particle might absorb some of the light, preventing it from reaching $Ru(bpy)_3^{2+}$, and therefore making steady-state quenching analysis unreliable. In order to overcome this, we used time-resolved photoluminescence spectroscopy, since photoluminescence lifetime is not sensitive to the intensity of the excitation light but it is sensitive to quenching by photoinduced electron transfer reactions. Fig. 5 shows the time-resolved transients for Ru-MCM-41 and Ru-pSWCNTs@MCM-41. The red curve represents the slowly decaying photoluminescence of Ru-MCM-41 showing a biexponential decay with lifetimes of 186 and 681 ns; Ru-pSWCNTs@MCM-41 photoluminescence decay can also be fitted to a biexponential decay with lifetimes of 8.2 and 600 ns. The 8.2 short lifetime can be attributed to quenching of Ru$(bpy)_3^{2+}$ inside the MCM-41 channels but that are near the surface, in close proximity to SWCNTs. The long lifetime observed is probably due to $Ru(bpy)_3^{2+}$ that are buried inside the channels of the MCM-41 particle and therefore farther away from the SWCNTs. Since little or no quenching occurs for these complexes, the lifetime is closer to that of Ru-MCM-41. Binding of $Ru(bpy)_3^{2+}$ to SWCNTs on the surface is not likely, first because the positive charge of pSWCNTs would repel $Ru(bpy)_3^{2+}$ dications, and secondly because previous studies from our laboratory have shown that $Ru(bpy)_3^{2+}$ has little affinity for SWCNTs.[47] To the best of our knowledge, this is the first time that photoinduced electron transfer to protonated SWCNTs has been reported. This data presents a proof-of-concept of a novel application of these materials, especially, considering the large

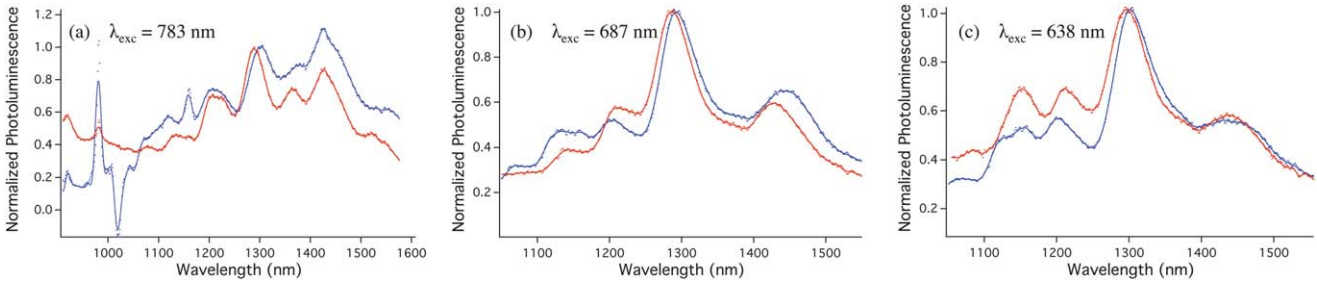

Fig. 4 Photoluminescence spectra of vpSWCNTs@MCM-41 0.67% (w/w) (—) and SWCNTs dispersed in NMP (—).

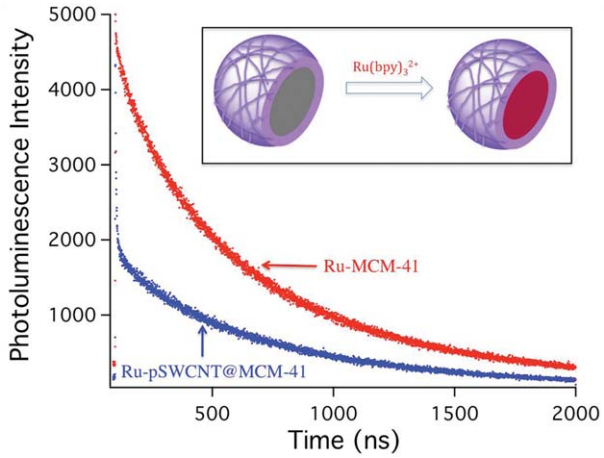

Fig. 5 Time-resolved photoluminescence decay for $Ru(bpy)_3^{2+}$ in MCM-41 (—) and pSWCNTs@MCM-41 (—). The samples were excited at 444 nm and emission was recorded at 620 nm.

amount of different molecules that can be immobilized in the internal cavities of these silicates. We propose that porous supramolecular framework materials present an alternative to study the interaction of SWCNTs with photoactive species immobilized in their internal framework. Since different zeolites and MCM-41 materials can be synthesized with tunable pore sizes, a large variety of photoactive molecules can be potentially used, for applications that range from catalysis to solar energy conversion. Furthermore, photoactive molecules can be studied using these scaffolds, without time consuming chemical modification with anchoring agents. Studies of $Ru(bpy)_3^{2+}$ with deprotonated vpSWCNTs@MCM-41 and its potential application to solar energy storage and conversion are currently underway and will be reported soon.

Conclusion

In conclusion, we report the immobilization of individual SWCNTs on the surface of microporous and mesoporous silicate materials using CSA. Spectroscopic studies demonstrate that these materials are covered with mostly individual protonated SWCNTs. Treatment with VP deprotonates the SWCNTs and prevents their aggregation, as shown by Raman, diffuse reflectance, and near-infrared photoluminescence emission from these materials. Notably, the recovery of photoluminescence from functionalized SWCNTs deposited on MCM-41 is novel, and combined with the high surface area and porosity of these zeolitic materials, presents unique advantages that can be exploited in the construction of new hybrid materials with interesting physical and electronic properties. Furthermore, the possibility of immobilizing photoactive species such as $Ru(bpy)_3^{2+}$ within the channels and cavities of these materials, provides an easy way to study their interaction with SWCNTs on the surface without the need of anchoring molecules. This is an example of how supramolecular systems can be combined with nanomaterials to produce novel hybrid materials with interesting properties.

Acknowledgements

We thank Dr Noe Alvarez, and Professor James Tour for helpful suggestions and the Welch Foundation (L-C-0003, C-1743, and C-1668) for financial support.

Notes and references

1 L. J. Carlson and T. D. Krauss, *Acc. Chem. Res.*, 2008, **41**, 235–243.
2 P. M. Ajayan, *Chem. Rev.*, 1999, **99**, 1787–1799.
3 D. Tasis, N. Tagmatarchis, A. Bianco and M. Prato, *Chem. Rev.*, 2006, **106**, 1105–1136.
4 R. C. Haddon, *Acc. Chem. Res.*, 2002, **35**, 997.
5 M. C. Hersam, *Nat. Nanotechnol.*, 2008, **3**, 387–394.
6 H. Dai, *Acc. Chem. Res.*, 2002, **35**, 1035–1044.
7 S. Iijima and T. Ichihashi, *Nature*, 1993, **363**, 603–605.
8 D. S. Bethune, C. H. Kiang, M. S. de Vries, G. Gorman, R. Savoy, J. Vazquez and R. Beyers, *Nature*, 1993, **363**, 605–607.
9 S. Reich, C. Thomsen and J. Maultzsch, *Carbon Nanotubes. Basic Concepts and Physical Properties*, Wiley-VCH, Weinheim, 2004.
10 O. Zhou, H. Shimoda, B. Gao, S. Oh, L. Fleming and G. Yue, *Acc. Chem. Res.*, 2002, **35**, 1045–1053.
11 S. V. Rotkin and S. Subramoney, ed., *Applied Physics of Carbon Nanotubes. Fundamentals of Theory, Optics and Transport Devices*, Springer, Berlin, 2005.
12 S. Ramesh, H. Shan, E. Haroz, W. E. Billups, R. Hauge, W. W. Adams and R. E. Smalley, *J. Phys. Chem. C*, 2007, **111**, 17827–17834.
13 E. Menna, F. D. Negra, M. Prato, N. Tagmatarchis, A. Ciogli, F. Gasparrini, D. Misiti and C. Villani, *Carbon*, 2006, **44**, 1609.
14 Y. Li, Y. Chen, R. Xiang, D. Ciuparu, L. D. Pfefferle, C. Horváth and J. A. Wilkins, *Anal. Chem.*, 2005, **77**, 1398–1406.
15 M. Tang, Y. Qin, Y. Wang and Z.-X. Guo, *J. Phys. Chem. C*, 2009, **113**, 1666–1671.
16 T. Fujigaya, J. B. Yoo and N. Nakashima, *Carbon*, 2011, **49**, 468–476.
17 P. Hu, C. Z. Huang, Y. F. Li, J. Ling, Y. L. Liu, L. R. Fei and J. P. Xie, *Anal. Chem.*, 2008, **80**, 1819–1823.
18 J. Shi, Z. Chen, Y. Qin and Z.-X. Guo, *J. Phys. Chem. C*, 2008, **112**, 11617–11622.
19 R. Xu, W. Pang, J. Yu, Q. Huo and J. Chen, *Chemistry of Zeolites and Related Porous Materials. Synthesis and Structure*, Wiley, Singapore, 2007.
20 C. Baerlocher, W. M. Meier and D. H. Olson, *Atlas of Zeolite Framework Types*, Elsevier, 2001.

21 R. Krishna and J. M. van Baten, *Microporous Mesoporous Mater.*, 2008, **107**, 296–298.
22 M. Hunger, U. Schenk and A. Buchholz, *J. Phys. Chem. B*, 2000, **104**, 12230–12236.
23 J. S. Kim and M. A. Keane, *J. Colloid Interface Sci.*, 2000, **232**, 126–132.
24 P. Sun, S. Deore and A. Navrotsky, *Microporous Mesoporous Mater.*, 2006, **91**, 15–22.
25 B. Hennessy, S. Megelski, C. Marcolli, V. Shklover, C. Bärlocher and G. Calzaferri, *J. Phys. Chem. B*, 1999, **103**, 3340–3351.
26 J. R. Herance, E. Peris, J. Vidal, J. L. Bourdelande, J. Marquet and H. Gracía, *Chem. Mater.*, 2005, **17**, 4097–4102.
27 I. W. Chiang, B. E. Brinson, A. Y. Huang, P. A. Willis, M. J. Bronikowski, J. L. Margrave, R. E. Smalley and R. H. Hauge, *J. Phys. Chem. B*, 2001, **105**, 8297–8301.
28 R. Ryoo, C. H. Ko and I.-S. Park, *Chem. Commun.*, 1999, 1413–1414.
29 P. K. Rai, R. A. Pinnick, A. N. G. Parra-Vasquez, V. A. Davis, H. K. Schmidt, R. H. Hauge, R. E. Smalley and M. Pasquali, *J. Am. Chem. Soc.*, 2006, **128**, 591–595.
30 L. A. Girifalco, M. Hodak and R. S. Lee, *Phys. Rev. B: Condens. Matter*, 2000, **62**, 13104.
31 S. Ramesh, L. M. Ericson, V. A. Davis, R. K. Saini, C. Kittrell, M. Pasquali, W. E. Billups, W. W. Adams, R. H. Hauge and R. E. Smalley, *J. Phys. Chem. B*, 2004, **108**, 8794–8798.
32 V. A. Davis, L. M. Ericson, A. N. G. Parra-Vasquez, H. Fan, Y. Wang, V. Prieto, J. A. Longoria, S. Ramesh, R. K. Saini, C. Kittrell, W. E. Billups, W. W. Adams, R. H. Hauge, R. E. Smalley and M. Pasquali, *Macromolecules*, 2004, **37**, 154–160.
33 V. A. Davis, A. N. G. Parra-Vasquez, M. J. Green, P. K. Rai, N. Behabtu, V. Prieto, R. D. Booker, J. Schmidt, E. Kesselman, W. Zhou, H. Fan, W. W. Adams, R. H. Hauge, J. E. Fisher, Y. Cohen, Y. Talmon, R. E. Smalley and M. Pasquali, *Nat. Nanotechnol.*, 2009, **4**, 830–834.
34 D. S. Hecht, A. M. Heintz, R. Lee, L. Hu, B. Moore, C. Cucksey and S. Risser, *Nanotechnology*, 2011, **22**, 075201.
35 D. A. Heller, P. W. Barone, J. P. Swanson, R. M. Mayrhofer and M. S. Strano, *J. Phys. Chem. B*, 2004, **108**, 6905–6909.
36 M. J. O'Connell, S. Sivaram and S. K. Doorn, *Phys. Rev. B: Condens. Matter Mater. Phys.*, 2004, **69**, 235415.
37 Z. Luo, S. K. Doorn, R. Li and F. Papadimitrakopoulos, *Phys. Status Solidi B*, 2006, **243**, 3155–3160.
38 Z. Chen, K. Kobashi, U. Rauwald, R. Booker, H. Fan, W.-F. Hwang and J. M. Tour, *J. Am. Chem. Soc.*, 2006, **128**, 10568–10571.
39 B. C. Satishkumar, S. K. Doorn, G. A. Baker and A. M. Dattelbaum, *ACS Nano*, 2008, **2**, 2283–2290.
40 C. Zamora-Ledezma, L. Añez, J. Primera, P. Silva, S. Etienne-Calas and E. Anglaret, *Carbon*, 2008, **46**, 1253–1269.
41 A. N. G. Parra-Vasquez, Solubility, Lenght Characterization, and Cryo-TEMof Pristine and Functionalized Single-Walled Carbon Nanotubes in Surfactant and Superacid Systems With Application to Spinning SWNT Fibers, PhD Thesis, Rice University, Houston, 2009.
42 E. Maligaspe, A. S. D. Sandanayaka, T. Hasobe, O. Ito and F. D'Souza, *J. Am. Chem. Soc.*, 2010, **132**, 8158–8164.
43 F. D'Souza, A. S. D. Sandanayaka and O. Ito, *J. Phys. Chem. Lett.*, 2010, **1**, 2586–2593.
44 J. Yu, S. Mathew, B. S. Flavel, M. R. Johnston and J. G. Shapter, *J. Am. Chem. Soc.*, 2008, **130**, 8788–8796.
45 D. Baskaran, J. W. Mays, X. P. Zhang and M. S. Bratcher, *J. Am. Chem. Soc.*, 2005, **127**, 6916–6917.
46 E. Bottinelli, I. Miletto, G. Caputo, S. Coluccia and E. Gianotti, *J. Fluoresc.*, 2010, **21**, 901–909.
47 D. Jain, A. Saha and A. A. Martí, *Chem. Commun.*, 2011, **47**, 2246–2248.